

光学学报

基于直流偏置光正交频分复用的水下光通信自适应光强探测电路设计

任秀云, 李秀娜, 张延超*, 张志华, 欧阳辰穗, 唐子帆

哈尔滨工业大学(威海)信息科学与工程学院, 山东威海 264209

摘要 针对水下光通信受湍流、生物活动等影响引起链路失准, 或通信距离改变导致接收光强变化较大的问题, 结合直流偏置正交频分复用光信号的特点, 提出了一种自适应光强探测电路。该电路通过自动增益控制技术调整对接收信号的放大倍数, 输出稳定的电信号。首先对自适应光强探测电路的相关参数进行理论分析和仿真验证, 然后设计研制该电路并进行空气信道和水下信道的实验测试。结果表明, 该电路能够实现对不同强度光信号的自适应调节, 输出电信号峰峰值基本稳定在 600 mV 左右, 波动范围为 $-3.3\% \sim 3.3\%$ 。

关键词 水下光通信; 自适应光强探测; 自动增益控制; 对数放大电路

中图分类号 TN929.1 文献标志码 A

DOI: 10.3788/AOS230622

1 引言

随着人类水下探测活动的增加, 各设备间的数据交换量迅速增长, 人们对水下无线通信技术的需求进一步提高。相较其他技术, 光通信具有数据承载量大、传输速率高、延时低等优点^[1-3], 因此近年来水下无线光通信(UWOC)技术引起了广泛关注^[4], 逐渐应用于水下无线传感网络、水下自主航行器通信、对潜通信等领域, 发展潜力巨大^[5]。光接收机是 UWOC 系统中的重要组成部分, 主要包括光电转换模块、信号放大模块和信号解调模块, 这些模块的设计性能是影响通信系统通信距离、速率及误码率等通信性能的关键因素。考虑到 UWOC 系统的工作环境、通信距离改变以及湍流、生物活动等引起的链路失准都会对光传输造成影响, 导致接收光强有较大变化^[6-9], 接收机信号非线性失真或丢失, 因此, 光接收机一般使用可变增益放大电路来解决待测光信号的强度变化问题。现有的可变增益放大电路分为两类, 一类是文献[10-12]中采用的电路, 该电路利用低噪声固定增益前置放大器和限幅放大器实现两次放大输出, 然后信号进入判决器和时钟恢复电路进行数据恢复即时钟恢复和数据重定时, 其中限幅放大器决定了输出信号的幅值。这一类设计具有电路设计简单的优点, 但一般适用于采用开关键控调制、位置脉冲调制的数字传输光通信系统。此外, 正

交频分复用(OFDM)信号峰均功率比高, 若采用限幅放大器容易造成信号非线性失真, 降低系统性能。另一类可变增益放大电路则是采用自动增益控制(AGC)电路扩大光接收机探测信号的动态范围^[13-17]。文献[13-14]中的 AGC 电路使用检波器检测输出信号幅值变化, 进而构成增益控制反馈回路, 该电路具有结构简单、易于实现的优点。但是由于电路达到稳定工作状态的时间受反馈回路特性的影响、AGC 调节时间固定以及增益控制存在滞后等原因, 该电路不能处理高速高频信号。文献[15-16]利用单片机和算法控制可编程增益信号放大器的增益, 该方法的控制响应时间受单片机以及模-数转换和数-模转换的速度限制。所提自适应光强探测电路与以上方案相比具有响应速度快、实时性强的优点, 增益控制不存在滞后性, 可以较好地处理通信中的高频信号和数据帧。

为了有效提高无线光通信技术的通信速率, 近年来科研工作者在调制解调技术上进行了大量研究, 研究结果表明, 基于 OFDM 的调制解调技术能够有效提高频谱利用率, 从而提升无线光通信系统的通信速率^[18-24]。OFDM 技术应用于无线光通信系统主要有非对称限幅光 OFDM 和直流偏置光 OFDM(DCO-OFDM)两种形式, 其中 DCO-OFDM 技术因具有频谱利用率高、易于实现等优点而被广泛应用于 UWOC 系统^[25-27]。

收稿日期: 2023-03-02; 修回日期: 2023-04-06; 录用日期: 2023-04-17; 网络首发日期: 2023-05-08

基金项目: 国家重点实验室开放项目(SKLLIM 1915)、山东省重大科技创新工程(2020CXGC010705)、哈尔滨工业大学科学研究院与创新基金(ITDZMZ001803)

通信作者: *zhangyanchao66@sina.com

本文在分析得出 DCO-OFDM 调制的 UWOC 信号具有传输速率快、载波频段较高、数据存在帧结构、信号帧之间存在间隙等特点的基础上,采用电压控制型放大器 AD603 设计了一种自适应光强探测电路。该电路利用 DCO-OFDM 信号中直流信号与交流信号幅值成正比的特性,将直流信号进行对数放大,从而形成控制电压来调整交流放大电路的放大倍数。为了验证该电路对动态光信号的自适应调节效果,搭建了基于 DCO-OFDM 调制的激光通信实验系统,在接收端使用可调光阑改变接收光信号的强度。当接收信号强度改变,直流电压在 18~1300 mV 范围内变化时,输出电信号峰峰值基本稳定在 600 mV,波动范围为 -3.3%~3.3%,自适应光强探测电路的增益调整范围为 6.8~30.0 dB。结果表明,该电路可以自适应地调节对不同强度光信号的放大倍数,扩大水下光通信系统接收机的动态范围。

2 基于 DCO-OFDM 调制信号的自动增益控制

图 1 是示波器测量的 UWOC 系统进行以太网通信时的 OFDM 信号,其中:C2 是打包成不连续数据帧的 OFDM 信号;Z2 是放大的 OFDM 波形细节。由图 1 可见,OFDM 信号的时域波形幅值变化较大,且传输信号被打包成数据帧,以太网传输速率不同时,相邻两帧之间存在的帧间隙大小不一。帧间隙的存在是因为接收机在接收一帧数据后需要一段时间来处理信号(如调整缓存取的指针、更新计数等)并为接收下一帧作准备。传统 AGC 电路将检波器输出信号作为增益控制电压形成反馈回路,AGC 环路时间常数与输入信号幅值、检波器检波特性等有关,不能灵活地适应 OFDM 帧间隙的出现和不同帧段的幅度变化。若时间常数过大,则输入信号发生变化一段时间后自动增益控制才能发挥作用,AGC 电路反应滞后,不能快速响应通信中 OFDM 数据帧的变化,容易造成信号饱和或过小;若时间常数过小,则 OFDM 数据帧中不同帧段的正常幅度变化会被抑制,容易出现反调制。

考虑光信号的非负特性,UWOC 需要在 OFDM 信号上增加直流偏置使传输信号恒为正,即 DCO-OFDM 信号。显然,DCO-OFDM 信号中同时含有直流信号和交流信号。经过信道传输后,光信号强度受信道影响会有较大变化,但交流信号和直流偏置信号是同步衰减的^[28],其比例关系保持不变。因此,可以利用直流信号形成控制电压来调整交流通路的电路增益,从而保证交流信号的稳定传输。

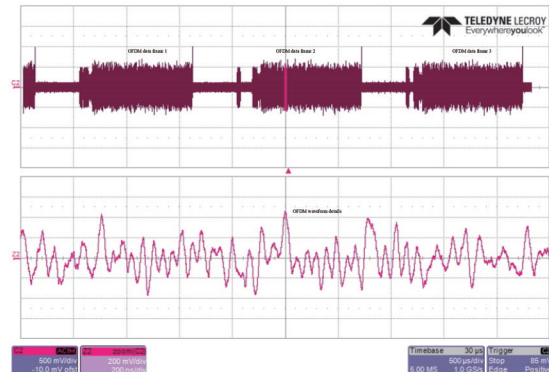


图 1 以太网通信中的 OFDM 信号
Fig. 1 OFDM signals in ethernet communications

图 2 是基于 DCO-OFDM 的自适应光强探测电路原理图。UWOC 系统发射机中的驱动调制电路将直流偏压与 OFDM 调制形成的交流信号耦合后形成 DCO-OFDM 信号,进而驱动激光二极管(LD)发射光信号。根据测得的光源光功率-电流特性,保证光源工作在线性区,从而确定直流偏置的大小。经过信道传输衰减后,接收机的 PIN(positive-intrinsic-negative)光电探测器将光信号转换为电信号。电信号的直流信号经过固定增益放大器和对数放大器后形成控制电压,以控制可变增益放大电路的放大倍数;交流信号经跨阻放大器放大后进入可变增益放大电路被二级放大,然后进入解调器解调。最后,在 PC(personal computer)机上恢复出原始信号。该电路可以根据接收光信号的强度快速自动调整交流信号的总放大倍数,实现数据信号的稳定传输。

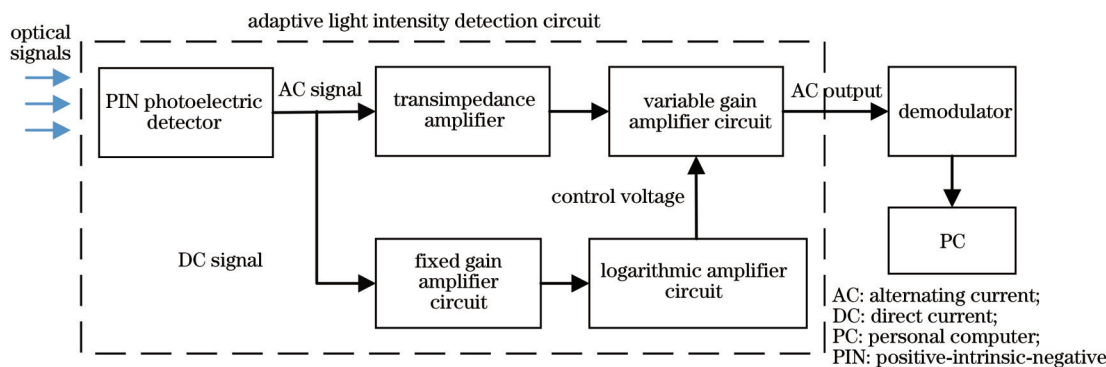


图 2 基于 DCO-OFDM 的自适应光强探测电路原理图
Fig. 2 Schematic diagram of adaptive light intensity detection circuit based on DCO-OFDM

3 基于 DCO-OFDM 的自适应光强探测电路设计

自适应光强探测电路由光电探测器、跨阻放大器、可变增益放大电路、固定增益放大电路及对数放大电路组成,整体设计如图 3 所示。

PIN 光电探测器输出的直流电压 V_{DC} 经过固定增益放大电路和对数放大电路形成控制压差电压 V_{o4} ,以控制可变增益放大器 AD603 的增益值。电路增益 $A_{Gain}(\text{dB})$ 与 AD603 增益控制电压 V_G 的关系表示为

$$A_{Gain} = 40 \times V_G + 10, \quad (1)$$

式中, $V_G = V_{o4} - V_{set}$, 其中 V_{set} 为可设置电压, 在本设计中 $V_{set} = 5.5 \text{ V}$ 。

PIN 光电探测器输出的交流电流经跨阻放大器转换为交流电压 V_i , 再经可变增益放大电路进行二次放大, 放大后为 V_o 。令 $A = V_o/V_i$, 则 $A_{Gain} = 20\lg(A)$ 。由式(1)可以推导出可变增益放大器 AD603 的控制电压与电路放大倍数的关系为

$$V_G = \frac{1}{2} \times \lg A - \frac{1}{4}. \quad (2)$$

对数放大电路采用德州仪器推出的精密高速对数运算放大器 LOG114, 该对数运算放大器的输出电压表示为

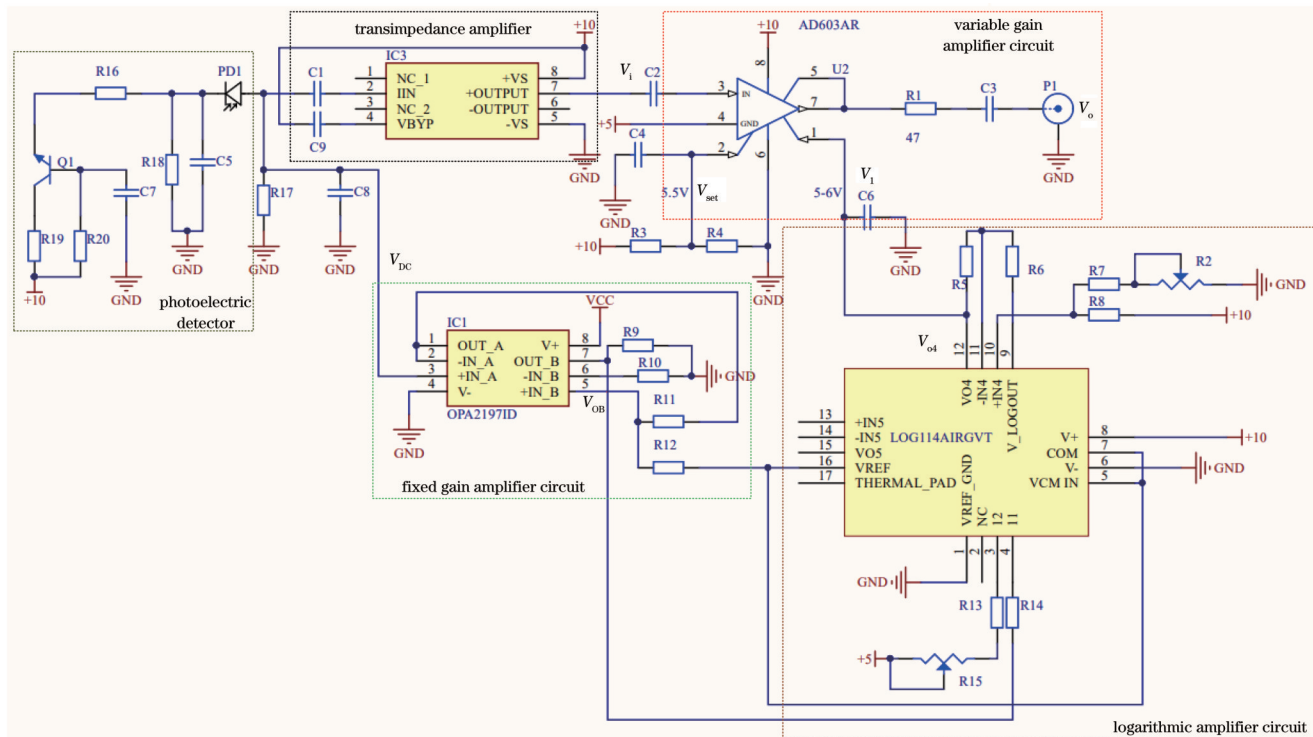


图 3 自适应光强探测电路图
Fig. 3 Adaptive light intensity detection circuit diagram

4 实验验证与结果分析

4.1 实验装置

激光通信系统实验设置如图 4 所示。OFDM 信号

$$V_{LOGOUT} = 0.375 \times \lg \left(\frac{I_1}{I_2} \right) + V_{com}, \quad (3)$$

式中: I_1 为输入信号产生的电流, $I_1 = \frac{V_{OB} - V_{com}}{R_{14}}$ (V_{OB} 为固定增益放大电路的输出电压); $I_2 = \frac{2.5}{R_{13} + R_{15}}$; V_{com} 为连接到 com 引脚的偏置电压, $V_{com} = 2.5 \text{ V}$ 。令电压 V_{LOGOUT} 经过 LOG114 集成运算放大器进行反向放大并增加直流偏置, 得到 V_{o4} , 表示为

$$\begin{aligned} V_{o4} = & -\frac{R_5}{R_6} V_{LOGOUT} + \left(1 + \frac{R_5}{R_6} \right) \times V_{REF} = \\ & -\frac{R_5}{R_6} \left\{ 0.375 \times \lg \left[\frac{V_{DC}/R_{14}}{2.5/(R_{13} + R_{15})} \right] + 2.5 \right\} + \\ & \left(1 + \frac{R_5}{R_6} \right) \frac{R_2 + R_7}{R_2 + R_7 + R_8} \times 10, \end{aligned} \quad (4)$$

式中, V_{REF} 为 LOG114 集成运算放大器的内部电压基准, 用于调整运算放大器输出的直流偏移量。

联立式(1)、式(2)和式(4)可确定对数放大电路的参数, 设置 R_5 、 R_6 、 V_{REF} , 使可变增益放大电路可以处理一定动态范围的输入信号。可设置的增益控制范围为 $-10 \sim 30 \text{ dB}$, 自适应光强探测电路的输出电信号保持稳定。

由程序生成, 并加载到任意波形发生器(AWG)中, 有效子载波频段为 $5 \sim 45 \text{ MHz}$ 。AWG 输出的 OFDM 信号经过放大电路放大, 与直流偏置电压叠加, 驱动 450 nm LD 工作。为了获得能量分布均匀的发射激光

光束,首先让发射激光透过毛玻璃屏均匀散射^[29],然后由光学发射天线准直。在接收机一侧采用通光孔径为3~52 mm可调的光阑控制光通量改变,光学接收天线将光信号聚焦到PIN光电探测器光敏面上。PIN光电探测器将光信号转换为电信号,电信号进入跨阻放大器和可变增益放大电路。利用示波器对放大后的交流

信号进行观察和记录,利用数字万用表对直流信号进行测量。实际测试中空气信道的激光通信系统如图5所示,其中:发射机如图5(a)所示;接收端包括可调光阑、接收机[图5(b)]。在尺寸为60 cm×60 cm×60 cm的水箱中注入衰减系数为5.26 m⁻¹(450 nm)的浑浊水,作为水下信道信号传输的实验装置,如图6所示。

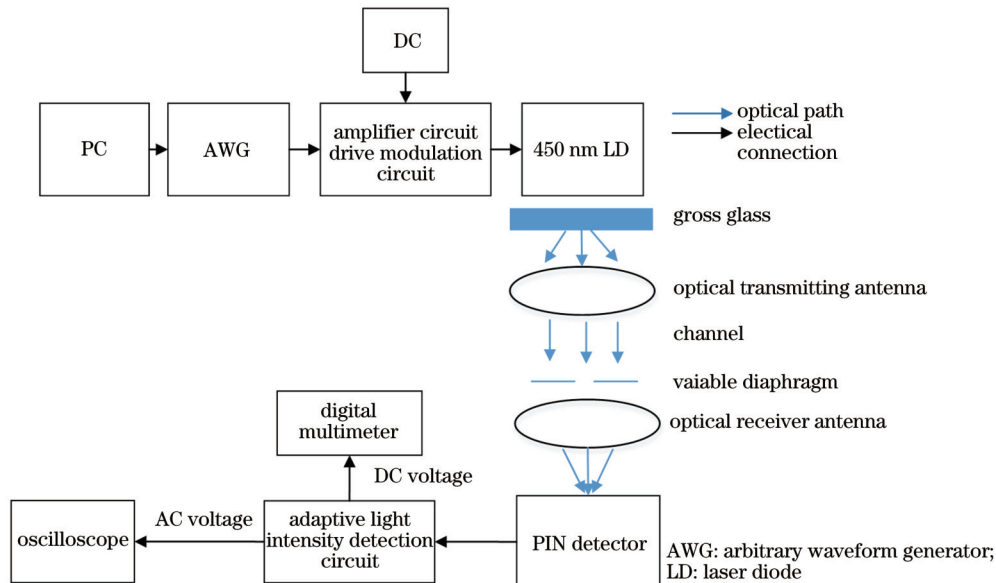


图4 激光通信系统实验设置
Fig. 4 Experimental setup of laser communication system

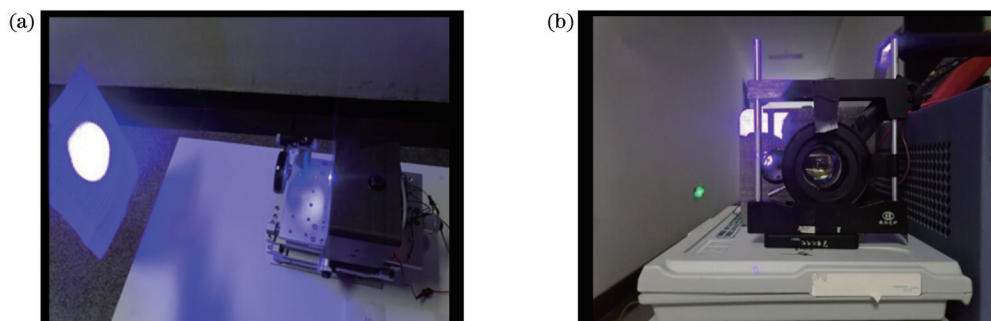


图5 激光通信系统实验装置。(a)发射机;(b)接收机
Fig. 5 Experimental equipments of laser communication systems. (a) Transmitter; (b) receiver

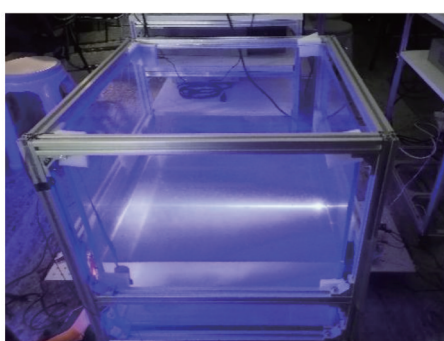


图6 水下信道的激光通信实验装置
Fig. 6 Laser communication experimental setup for underwater channels

4.2 实验结果及分析

4.2.1 DCO-OFDM 信号及电路参数分析

为了衡量可变光阑对接收光信号强度的改变情况,在可变光阑后利用光电池实验测量了不同通光孔径时的光电池短路电流。由文献[30-31]可知,光电池的短路电流与光照度成正比。根据ZL-G010硅光电池的数据手册(短路电流为100 lx, 20 μA)可以得到接收端的光照度,如表1所示。实验结果表明,可变光阑可以改变接收光信号强度,满足实验需求。

实验进一步测量了当光照度改变时,PIN输出的直流电压与经过跨阻放大器转换的交流信号峰峰值,如表2所示。由于光信号经过相同的信道衰减,DCO-OFDM 直流信号和交流信号同步衰减,它们之间的关

表1 接收端的光照强度

Table 1 Light intensity at the receiving end

| | | | | | | | | | | |
|---------------------------------|-------|-------|-------|-------|-------|-------|-------|-------|-------|-------|
| Short-circuit current / μ A | 23.0 | 31.0 | 40.0 | 56.0 | 59.4 | 60.2 | 69.0 | 70.0 | 71.5 | 81.4 |
| Illumination /lx | 115.0 | 155.0 | 200.0 | 280.0 | 297.0 | 301.0 | 345.0 | 350.0 | 357.5 | 407.0 |

系应保持不变。图7为当光阑孔径变化时直流信号和交流信号的线性拟合关系,其中:横坐标为直流电压 V_{DC} ;纵坐标为跨阻放大器输出的OFDM信号峰峰值,即交流电压 V_i ,两者间的关系表示为

表2 直流信号和输入交流信号测试数据

Table 2 Test data of DC signal and input AC signal

| | | | | | | | | | | |
|--|---|-----|-----|-----|-----|-----|-----|-----|-----|-----|
| DC voltage V_{DC} /mV | 0 | 110 | 220 | 246 | 350 | 570 | 620 | 720 | 790 | 820 |
| AC signal peak-to-peak value V_i /mV | 0 | 32 | 50 | 55 | 72 | 120 | 125 | 155 | 168 | 175 |

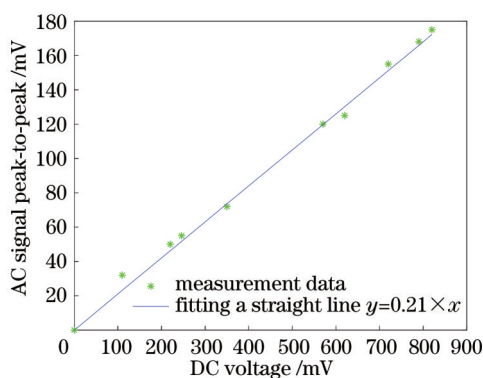


图7 直流信号、输入交流信号关系拟合图

Fig. 7 DC signal, input AC signal relationship fitting diagram

当光强改变、直流电压 V_{DC} 在18~1300 mV范围内变化时,考虑AGC电路增益调整范围和解调器可正常工作的接收信号范围,设计令自适应光强探测电路输出信号峰峰值 $V_o=600$ mV,联立式(4)和式(6)可得,当 $R_5/R_6=3.9/3.0$ 、 $V_{REF}=4.08$ V时,对数放大电路输出电压 V_{o4} 表示为

$$V_{o4}=-\frac{R_5}{R_6}V_{LOGOUT}+\left(1+\frac{R_5}{R_6}\right)V_{REF}=$$

表3 空气信道的光强自适应电路测试数据

Table 3 Light intensity adaptive circuit test data for air channel

| | | | | | | | | |
|--|------|------|------|------|------|------|------|------|
| DC voltage V_{DC} /mV | 110 | 220 | 246 | 350 | 570 | 620 | 720 | 790 |
| Logarithmic amplifier circuit output voltage V_{o4} /V | 5.91 | 5.76 | 5.74 | 5.67 | 5.57 | 5.55 | 5.52 | 5.50 |
| Transimpedance amplifier output AC signal (peak-to-peak) V_i /mV | 32 | 50 | 55 | 72 | 120 | 130 | 165 | 175 |
| AC output signal (peak-to-peak) V_o /mV | 600 | 580 | 600 | 620 | 600 | 590 | 600 | 600 |

根据测试数据 V_i 确定理想输出 V_o ,通过式(2)可以得到对应数据点的理论控制电压值。对数放大电路实际输出电压 V_{o4} 与理论分析计算得到的 V_i 如表4所示。图9是测量的直流信号与对数放大电路控制电压数据点的拟合曲线。如图9所示,对数放大电路产生的实际控制电压与由式(2)计算得到的理论控制电压基本一致,与理论值最大相差0.05 V。设计的对数放

$$V_i=0.21 \times V_{DC} \quad (5)$$

将式(5)代入式(2)可得

$$V_o=\frac{1}{2} \times \lg\left(\frac{V_o}{0.21V_{DC}}\right)-\frac{1}{4} \quad (6)$$

$$-0.49 \lg\left(\frac{V_{DC}/6.8 \times 10^3}{5.92 \times 10^{-6}}\right)+6.13, \quad (7)$$

AGC电路实际控制电压 V'_G 表示为

$$V'_G=V_{o4}-V_{set}=-0.49 \lg\left(\frac{V_{DC}/6.8 \times 10^3}{5.92 \times 10^{-6}}\right)+0.63. \quad (8)$$

4.2.2 自适应光强探测电路测试

1) 空气信道测试

确定对数放大电路参数后,测试了自适应光强探测电路处理信号的动态范围与输出信号的变化情况。表3记录了光信号强度改变时直流电压 V_{DC} 、控制压差电压 V_{o4} 、跨阻放大器输出信号峰峰值 V_i 以及可变增益放大电路输出信号峰峰值 V_o 的变化情况。由表3可见,虽然 V_{DC} 、 V_i 发生了较大变化,经放大输出后的信号峰峰值 V_o 始终保持在设定的600 mV左右。

图8中,通道2(粉色)为可变增益放大电路输出的交流信号,通道3(蓝色)为直流信号。可以看出,当光强改变、直流电压变化时,可变增益放大电路输出信号的幅值比较稳定。

大电路实现了预期功能:DCO-OFDM信号中的直流信号产生对交流信号的增益控制电压,从而调整自适应光强探测电路对交流信号的增益,使其输出幅值稳定的信号。

表5记录了理论分析得出的电路增益和测量的电路实际增益。图10为理想增益曲线与电路实际测试数据。由表5可以看出,该电路工作的实际增益与理

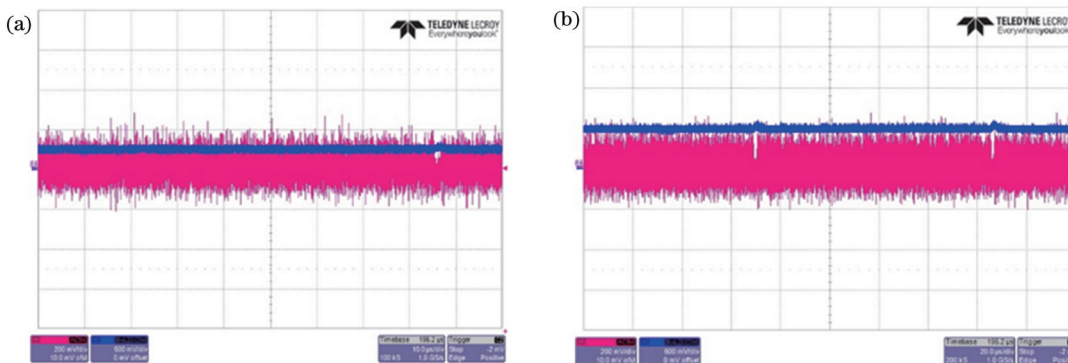


图8 信号强度改变时自适应光强探测电路的输出信号。(a) 直流信号为300 mV;(b) 直流信号为500 mV

Fig. 8 Adaptive light intensity detection circuit output signals when signal strength changes. (a) DC signal is 300 mV; (b) DC signal is 500 mV

表4 理论分析与电路实际控制信号数据

Table 4 Theoretical analysis and actual control signal data of the circuit

| DC voltage V_{DC} /mV | 110 | 220 | 246 | 350 | 570 | 620 | 720 | 790 |
|--|------|------|------|------|------|------|------|------|
| Logarithmic amplifier circuit output V_{o4} /V | 5.91 | 5.76 | 5.74 | 5.67 | 5.57 | 5.55 | 5.52 | 5.50 |
| Theoretical value V_1 /V | 5.86 | 5.76 | 5.74 | 5.68 | 5.57 | 5.55 | 5.51 | 5.49 |

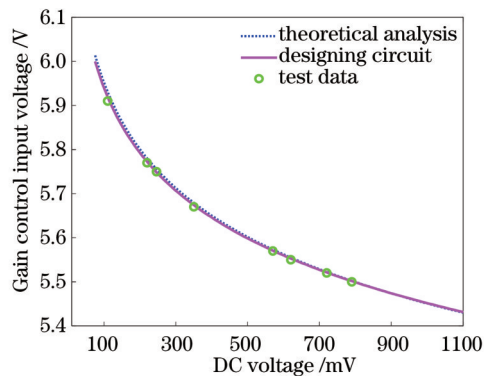


图9 直流信号-增益控制输入信号数据拟合曲线

Fig. 9 Fitting curves of DC signal-gain control input signal data

想增益最大相差0.62,即0.29 dB。该误差在可接受范围之内,说明所设计的自适应光强探测电路能较好地适应信号强度,自动调整电路增益。依据电路的硬件组成可以对该电路的响应时间作出估计,确定一个理论值。信号检测支路的延时时间为680 ns,AD603的增益控制响应时间约为1 μs,形成控制电压电路的响应时间约为0.25 μs,所以估计的整个电路的响应时间为1.93 μs。

在不同的光照强度下,自适应光强探测电路的输出情况如图11所示。随着光照强度改变,不同大小的

表5 电路实际增益与理想增益性能对比

Table 5 Comparison of actual gain and ideal gain performance of the circuit

| Actual gain | 18.13 | 11.60 | 10.91 | 8.61 | 5.00 |
|-------------|-------|-------|-------|-------|------|
| Ideal gain | 18.75 | 12.00 | 10.91 | 8.33 | 5.00 |
| Error | 0.62 | 0.40 | 0 | -0.28 | 0 |

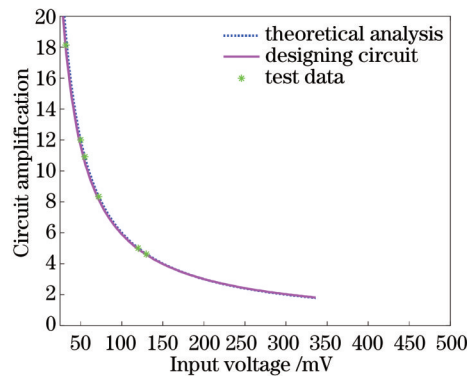


图10 电路放大倍数随输入信号的变化曲线

Fig. 10 Variation curves of circuit amplification with input signal

输入信号经自适应电路放大后,其输出峰峰值都能稳定在预设值600 mV左右,动态范围为-3.3%~3.3%,说明该电路具有光强自适应的优势,可以接收大动态范围的信号。

2)水下信道测试

令发射机和接收机分别位于尺寸为60 cm×60 cm×60 cm的玻璃水箱两侧,改变探测器的接收角度,测得的实验数据如表6所示。可以看出,当光信号经过水下信道、接收角度改变时,信号强度改变,自适应光强探测电路输出峰峰值在600 mV左右,比较稳定。

4.2.3 自适应光强探测电路用于激光通信系统的通信实验

在空气中对应用该自适应光强探测电路的蓝绿激光双向通信系统进行通信实验,通过改变通信距离、探测器接收角度来改变接收信号强度。激光通信系统的

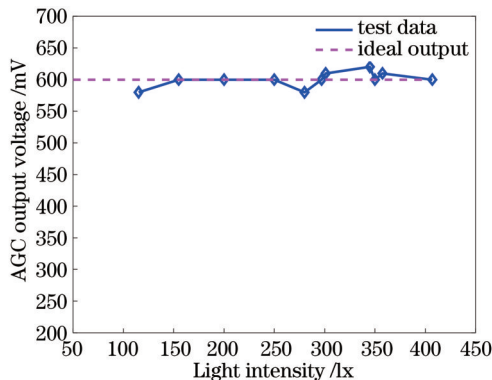


图 11 AGC 电路输出信号随光强的变化曲线

Fig. 11 Variation curves of AGC circuit output signal with light intensity

探测器、发射机相距 20 cm, 以激光通信系统发射机为原点, 改变探测器的接收角度。图 12 是当探测器位置改变时, 其直流电流变化, 其中: 图 12(a) 中光源为

450 nm LD(蓝光光源);图 12(b) 中光源为 520 nm LD(绿光光源)。当探测器与发射机相距 20 cm 时, 改变探测器接收角度, 蓝光探测器的直流电流在 0.66 μA~0.19 mA 范围内变化; 绿光探测器的直流电流在 0.47 μA~0.11 mA 范围内变化, 激光通信系统的通信速率约为 75 Mbit/s。

将发射机与接收机置于同一平面上的同一直线上, 如图 13 所示。在 20 cm~6 m 的距离范围内, 可成功建立通信。当通信距离为 6 m 时, 通信速率约为 45 Mbit/s, 如图 14 所示。

当通信距离和探测器接收角度变化时, 自适应电路的输出基本能稳定在期望值附近, 表明该自适应光强探测电路在接收机处理动态信号的过程中较好地发挥了自适应的作用, 在一定程度上减少了通信距离改变和链路失准对激光通信系统的影响, 能够为复杂环境中的激光通信提供硬件保障。

表 6 水下信道的光强自适应电路测试数据

Table 6 Light intensity adaptive circuit test data for underwater channel

| DC voltage V_{DC} / mV | 356 | 441 | 480 | 593 | 620 | 660 | 759 | 828 | 890 |
|---|------|------|------|------|------|------|------|------|------|
| Logarithmic amplifier circuit output voltage V_{o4} / V | 5.52 | 5.47 | 5.45 | 5.40 | 5.39 | 5.38 | 5.35 | 5.33 | 5.32 |
| Transimpedance amplified output AC signal (peak-to-peak) V_i / mV | 200 | 230 | 220 | 300 | 300 | 310 | 370 | 400 | 410 |
| AC output signal (peak-to-peak) V_o / mV | 620 | 600 | 610 | 600 | 610 | 620 | 600 | 610 | 600 |

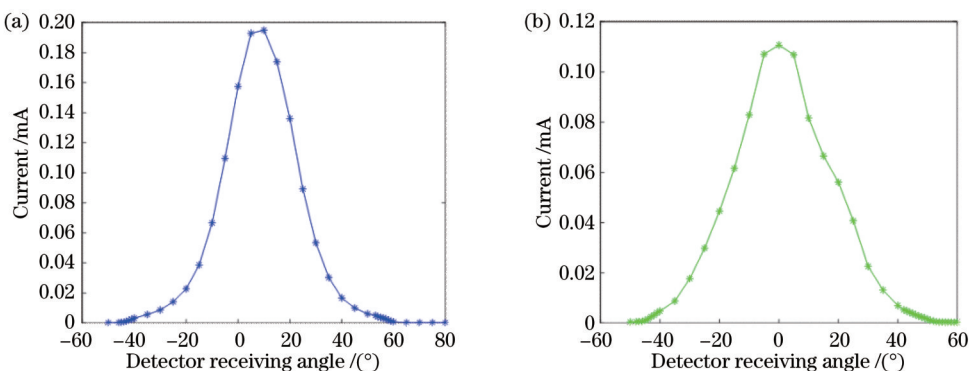


图 12 探测器直流电流与接收角度的关系。(a) 450 nm LD; (b) 520 nm LD

Fig. 12 Detector DC current versus receiving angle. (a) 450 nm LD; (b) 520 nm LD

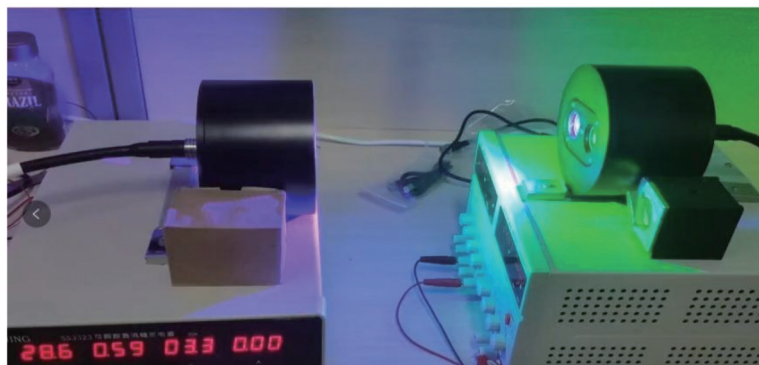


图 13 通信距离为 20 cm 时的激光通信系统

Fig. 13 Laser communication system at a communication distance of 20 cm



图14 通信距离为6 m时测量的传输速率

Fig. 14 Transmission rate measured at a communication distance of 6 m

5 结 论

基于采用DCO-OFDM调制的水下光通信系统信号特点,设计了一种直流信号经对数放大电路形成可变增益放大电路控制电压的自适应光强探测电路。将该电路应用到水下无线光通信系统中进行了空气信道和水下信道的通信实验。结果表明,当光信号强度改变时,直流电压在18~1300 mV范围内变化时,自适应光强探测电路输出信号峰峰值稳定在600 mV左右,波动范围为-3.3%~3.3%,实际工作增益与理想增益最大相差0.29 dB,激光通信系统可以建立通信。该自适应光强探测电路能够实现增益的自动调整,输出稳定信号,满足UWOC系统后续信号处理的要求,扩大了接收机接收光信号的动态范围,提高了UWOC系统在复杂信道环境下工作的可靠性。利用直流信号实现对交流信号增益控制的自适应光强探测电路具有结构简单、响应速度快、电路成本低、输出信号波动小的优势,有望广泛应用到无线光通信接收机中,进一步提升系统性能。

参 考 文 献

- [1] Xu J. Underwater wireless optical communication: why, what, and how? [J]. Chinese Optics Letters, 2019, 17(10): 100007.
- [2] Chitre M, Shahabdeen S, Stojanovic M. Underwater acoustic communications and networking: recent advances and future challenges [J]. Marine Technology Society Journal, 2008, 42(1): 103-116.
- [3] 万超, 郝浩, 赵清源, 等. 单光子探测在无线光通信收发技术中的应用 [J]. 激光与光电子学进展, 2022, 59(5): 0500001. Wan C, Hao H, Zhao Q Y, et al. Application of single photon detection in wireless optical communication transceiver technology [J]. Laser & Optoelectronics Progress, 2022, 59(5): 0500001.
- [4] 曾凤娇, 杨康建, 晏旭, 等. 水下激光通信系统研究进展 [J]. 激光与光电子学进展, 2021, 58(3): 0300002. Zeng F J, Yang K J, Yan X, et al. Research progress of underwater laser communication system [J]. Laser & Optoelectronics Progress, 2021, 58(3): 0300002.
- [5] Kaushal H, Kaddoum G. Underwater optical wireless communication [J]. IEEE Access, 2016, 4: 1518-1547.
- [6] Al-Kinani A, Wang C X, Zhou L, et al. Optical wireless communication channel measurements and models [J]. IEEE Communications Surveys & Tutorials, 2018, 20(3): 1939-1962.
- [7] 郝东, 李碧丽, 杨祎, 等. 水下无线光通信信道传输特性研究 [J]. 自动化与仪器仪表, 2021, 9: 21-24. Hao D, Li B L, Yang Y, et al. Research on transmission characteristics of underwater wireless optical communication channel [J]. Automation & Instrumentation, 2021, 9: 21-24.
- [8] Zeng Z Q, Fu S, Zhang H H, et al. A survey of underwater optical wireless communications [J]. IEEE Communications Surveys & Tutorials, 2017, 19(1): 204-238.
- [9] 李军, 罗江华, 元秀华. 水表面波扰动对无线光通信影响 [J]. 光学学报, 2021, 41(7): 0706005. Li J, Luo J H, Yuan X H. Influence of water surface wave disturbance on wireless optical communication [J]. Acta Optica Sinica, 2021, 41(7): 0706005.
- [10] Li Y F, Yin H X, Ji X Y, et al. Design and implementation of underwater wireless optical communication system with high-speed and full-duplex using blue/green light [C]//2018 10th International Conference on Communication Software and Networks (ICCSN), July 6-9, 2018, Chengdu, China. New York: IEEE Press, 2018: 99-103.
- [11] Kumar A, Naik R P, Acharya U S. Experimental studies on realization of underwater optical communication link [C]//2017 International Conference on Trends in Electronics and Informatics (ICEI), May 11-12, 2017, Tirunelveli, India. New York: IEEE Press, 2018: 708-712.
- [12] Kong M W, Guo Y J, Alkhazragi O, et al. Real-time optical-wireless video surveillance system for high visual-fidelity underwater monitoring [J]. IEEE Photonics Journal, 2022, 14(2): 7315609.
- [13] 高俊, 张玉兴. 使用AD603和AD8318实现大动态范围IF接收机 [J]. 现代电子技术, 2006, 29(5): 25-27. Gao J, Zhang Y X. Design a big dynamic range IF receiver with AD603 and AD8318 [J]. Modern Electronics Technique, 2006, 29(5): 25-27.
- [14] 谢生, 邱博文, 毛陆虹, 等. 可控增益光电集成光接收机设计 [J]. 天津大学学报, 2020, 53(8): 833-839. Xie S, Qiu B W, Mao L H, et al. Optoelectronic integrated optical receiver with automatic gain control [J]. Journal of Tianjin University, 2020, 53(8): 833-839.
- [15] 汪锋, 孙开江, 向小梅. 基于光电倍增管的自动增益控制技术研究 [J]. 激光技术, 2015, 39(4): 510-514. Wang F, Sun K J, Xiang X M. Research of automatic gain control technology based on photomultipliers [J]. Laser Technology, 2015, 39(4): 510-514.

- [16] 赵太飞, 杨黎洋, 袁麓, 等. 基于光电倍增管的自动增益放大器设计[J]. 光通信技术, 2017, 41(10): 5-8.
Zhao T F, Yang L Y, Yuan L, et al. Design of automatic gain amplifier based on photomultiplier[J]. Optical Communication Technology, 2017, 41(10): 5-8.
- [17] 周畅, 于笑楠, 姜会林, 等. 基于APD自适应增益控制的近地无线激光通信信道大气湍流抑制方法研究[J]. 中国激光, 2022, 49(4): 0406002.
Zhou C, Yu X N, Jiang H L, et al. Research on atmospheric turbulence suppression method of near-earth wireless laser communication channel based on APD adaptive gain control[J]. Chinese Journal of Lasers, 2022, 49(4): 0406002.
- [18] Fan Y Y, Green R J. Comparison of pulse position modulation and pulse width modulation for application in optical communications[J]. Optical Engineering, 2007, 46(6): 065001.
- [19] Jaruwatanadilok S. Underwater wireless optical communication channel modeling and performance evaluation using vector radiative transfer theory[J]. IEEE Journal on Selected Areas in Communications, 2008, 26(9): 1620-1627.
- [20] Shen C, Guo Y J, Oubei H M, et al. 20-meter underwater wireless optical communication link with 1.5 Gbps data rate[J]. Optics Express, 2016, 24(22): 25502-25509.
- [21] Ghassemlooy Z, Popoola W, Rajbhandari S. Optical wireless communications: system and channel modelling with MATLAB [M]. 2nd ed. Boca Raton: CRC Press/Taylor & Francis Group, 2019.
- [22] Rajagopal S, Roberts R D, Lim S K. IEEE 802.15.7 visible light communication: modulation schemes and dimming support [J]. IEEE Communications Magazine, 2012, 50(3): 72-82.
- [23] Nakamura K, Mizukoshi I, Hanawa M. Optical wireless transmission of 405 nm, 1.45 Gbit/s optical IM/DD-OFDM signals through a 4.8 m underwater channel[J]. Optics Express, 2015, 23(2): 1558-1566.
- [24] 王博, 吴琼, 刘立奇, 等. 水下无线光通信系统研究进展[J]. 激光技术, 2022, 46(1): 99-109.
Wang B, Wu Q, Liu L Q, et al. Research progress on the underwater wireless optical communication system[J]. Laser Technology, 2022, 46(1): 99-109.
- [25] Jean A. OFDM for optical communications[J]. Journal of Lightwave Technology, 2009, 27(3): 189-204.
- [26] Dissanayake S, Armstrong J. Comparison of ACO-OFDM, DCO-OFDM and ADO-OFDM in IM/DD systems[J]. Journal of Lightwave Technology, 2013, 31(7): 1063-1072.
- [27] Barrami F, Le Guennec Y, Novakov E, et al. An optical power efficient asymmetrically companded DCO-OFDM for IM/DD systems[C]//2014 23rd Wireless and Optical Communication Conference (WOCC), May 9-10, 2014, Newark, NJ, USA. New York: IEEE Press, 2014.
- [28] Cochenour B, Mullen L, Muth J. Temporal response of the underwater optical channel for high-bandwidth wireless laser communications[J]. IEEE Journal of Oceanic Engineering, 2013, 38(4): 730-742.
- [29] 孙嵘, 罗振坤, 赵映雪, 等. 两种激光散斑均化方法研究[J]. 激光与红外, 2010, 40(5): 455-458.
Sun R, Luo Z K, Zhao Y X, et al. Study of two methods to average the laser energy based on speckle interferometry[J]. Laser & Infrared, 2010, 40(5): 455-458.
- [30] 陈征, 王忠义, 欧阳祖熙. 光电池光强测量数字传感器设计[J]. 控制工程, 2010, 17(S3): 173-175.
Chen Z, Wang Z Y X, Ouyang Z. Photocell digital light intensity sensor design[J]. Control Engineering of China, 2010, 17(S3): 173-175.
- [31] 陈颖墨, 沈司熠, 王洁. 硅光电池的特性研究[J]. 大学物理实验, 2020, 33(1): 34-36.
Chen Y M, Shen S Y, Wang J. Study on the characteristics of silicon photocells[J]. Physical Experiment of College, 2020, 33(1): 34-36.

Design of Adaptive Light Intensity Detection Circuit for Underwater Optical Communication Based on Direct-Curren-Biased Optical Orthogonal Frequency Division Multiplexing

Ren Xiuyun, Li Xiuna, Zhang Yanchao^{*}, Zhang Zhihua, Ouyang Chensui, Tang Zifan

School of Information Science and Engineering, Harbin Institute of Technology, Weihai, Weihai 264209,

Shandong, China

Abstract

Objective With the expanding marine exploitation, high-speed long-reach underwater wireless communication has caught extensive attention. Compared with underwater acoustic communication and radio frequency communication, underwater wireless optical communication (UWOC) features a high data rate, great confidentiality, and large data capacity. Nevertheless, the challenging underwater environment exerts a significant effect on underwater light transmission. Absorption, scattering, and communication distance change may lead to a great variety of detection optical intensity, and the link misalignment between the transmitter and receiver caused by turbulence can also realize this. Nonlinear distortion or loss of receiver signal will be resulted in. Optical receivers generally employ variable gain amplification circuits to process dynamic signals to mitigate these effects. However, existing UWOC systems have some shortcomings. Limiting amplifier is generally applicable to optical communication systems of on-off keying modulation digital transmission. Automatic gain control (AGC) circuit generally adopts a detector to detect the changes in output signal amplitude to form a gain control feedback loop. In this feedback loop, the time to reach a stable operating state is affected by its characteristics,

and the AGC adjustment time is fixed, with hysteresis in gain control. We propose an adaptive light intensity detection circuit, which utilizes automatic gain control technology to adjust the amplification of the received signal and output stable electrical signals. This adaptive light intensity detection circuit has the advantages of fast response time and better real-time performance. We hope that our proposed method can improve the practicality of UWOC systems, aiming for optical communication systems in complex environments.

Methods Our proposed circuit is based on the characteristics of the direct-current-biased optical orthogonal frequency division multiplexing (DCO-OFDM) signal. The circuit takes advantage of the proportional relationship between the amplitude of the DC signal and the AC signal in the DCO-OFDM signal, and logarithmically amplifies the DC signal to form a control voltage to adjust the amplification of the AC amplifier circuit. The circuit leverages the AGC technique to adjust the amplification of the received signal and output a stable electrical signal. First, relevant parameters of the adaptive light intensity detection circuit are analyzed theoretically and verified by simulations, and then the circuit is designed and tested experimentally for air and underwater channels. The output signal of the adaptive light intensity detection circuit and the relationship between the control voltage formed by the logarithmic amplifier circuit and the gain of the circuit are investigated and compared with theoretical values. Then, this circuit is applied to an optical communication system for ethernet communication experiments at different distances.

Results and Discussions Our proposed circuit can realize automatic gain adjustment to output stable electrical signals, thereby expanding the optical communication system receiver's dynamic range of signal processing. Preliminary experiments are carried out to obtain the relationship between the AC signal and DC signal (Fig. 7). According to this relationship, we adjust the parameters of the designed circuit and further investigate the performance of the UOWC system through this circuit. The results of the air channel experiment show that when the light intensity changes, and the DC voltage varies from 18 mV to 1300 mV, and the output signal's peak-to-peak value in the variable gain amplifier circuit can be stabilized around the set value with a fluctuation range of $-3.3\%-3.3\%$ (Table 3). As depicted in Figs. 8(a) and 8(b), when the DC signal changes, the AC signal is stable. Then the logarithmic amplifier circuit's parameters are tested. Table 4 lists the theoretical and measured values of the control voltage. The results show that the designed logarithmic amplifier circuit realizes the desired function. The DC signal in the DCO-OFDM signal generates a gain control voltage to the AC signal (Fig. 9). Experiments for the underwater channel indicate that when the communication link is misaligned and the signal strength changes, the DC signal varies in the range of 356–890 mV and the peak-to-peak value of output signal is stable with a fluctuation range of $-3.3\%-3.3\%$ (Table 6). Finally, we experimentally demonstrate a 45 Mbit/s optical communication link over a 6 m air channel through the adaptive light intensity circuit in an optical communication system receiver (Fig. 14).

Conclusions We design an adaptive light intensity detection circuit based on the characteristics of the signal from an underwater optical communication system using DCO-OFDM modulation. The performance of the optical communication system in terms of received signals is experimentally analyzed for air and water as channel media. The feasibility of the circuit is demonstrated and verified in the experiment. The optical communication system which adopts an adaptive light intensity circuit shows good communication performance and robustness in various channels. When channel conditions such as link misalignment change, the peak-to-peak value of the circuit output signal is stable, and the maximum difference between the actual working gain and the ideal gain of the circuit is 0.29 dB. It is inferred from the experimental results that the circuit has better processing capability for dynamic signals. The adaptive optical intensity detection circuit employs DC signals to achieve gain control of AC signals with the advantages of simple structure, fast response, low circuit cost, and low output signal fluctuation. Additionally, it is expected to be widely applied in optical communication receivers to improve system performance.

Key words underwater optical communication; adaptive light intensity detection; automatic gain control; logarithmic amplifier circuit